Research Journal of Environmental Sciences

ISSN 1819-3412

Academic
Journals Inc.

www.academicjournals.com

OPEN ACCESS Research Journal of Environmental Sciences

ISSN 1819-3412
DOI: 10.3923/rjes.2017.116.129

Research Article
Kinetic and Thermodynamic Studies for the Removal of Cr(VI) from Aqueous Solutions Using Phosphonic Acid Functionalized Multiwalled Carbon Nanotubes

[1]Tarisai Velempini, [1,2]Kriveshini Pillay and [1]Xavier Y. Mbianda

[1]Department of Applied Chemistry, University of Johannesburg, Doornfontein Campus, P.O. Box 17011, Johannesburg, South Africa
[2]DST/NRF Centre of Excellence in Strong Materials, Johannesburg, South Africa

Abstract

Background and Objective: Multiwalled carbon nanotubes functionalized with 2-aminoethylphosphonic acid denoted phosphorylated multiwalled carbon nanotubes, (P-MWCNTs) were synthesized by first oxidizing pristine MWCNTs to obtain a number of functional groups which included carboxylic acids. The carboxylic acids were reacted with oxalyl chloride to obtain acyl chloride (-COCl). The 2-aminoethylphosphonic acid (AMP) was subsequently grafted onto acyl chloride (-COCl). This study aimed to report, the recovery of lowly concentrated Cr(VI) ions from aqueous solutions by using phosphorylated multiwalled carbon nanotubes (P-MWCNTs). **Materials and Methods:** The material was characterised by various techniques, including scanning electron microscopy (SEM), Fourier transform infrared spectroscopy (FTIR), Raman spectroscopy and thermo gravimetric analysis (TGA). The effectiveness of P-MWCNTs as an adsorbent for the removal of Cr(VI) from aqueous solutions were studied in a batch mode. To ensure that the data was reliable all batch adsorption experiments were carried out in triplicate. The standard deviation of the triple analytical data was determined and probability level used was $\leq$5%. **Results:** The results indicated a maximum adsorption of 93% at a pH of 2. Other parameters such as adsorbent dosage, contact time, initial ion concentration, temperature and the presence of competing ions were also investigated. The adsorption equilibrium was reached after 60 min and uptake decreased with initial anion concentration increments. Both Langmuir and Freundlich isotherms were applied to describe Cr(VI) adsorption process and Freundlich isotherm correlated well with the adsorption data. The adsorption reaction followed pseudo-second-order kinetics under different initial ion concentration, while removal percentage increased with increase in temperature. **Conclusion:** The enthalpy Gibbs free energy revealed that the adsorption process is endothermic (G<0) and spontaneous, as confirmed by standard enthalpy (S>0). Furthermore, regeneration of the adsorbent was successfully demonstrated with 1.0 M NaOH.

Key words: Multiwalled carbon nanotubes, adsorption, chromium(VI), kinetic, thermodynamic

Citation: Tarisai Velempini, Kriveshini Pillay and Xavier Y. Mbianda, 2017. Kinetic and thermodynamic studies for the removal of Cr(VI) from aqueous solutions using phosphonic acid functionalized multiwalled carbon nanotubes. Res. J. Environ. Sci., 11: 116-129.

Corresponding Author: Xavier Y. Mbianda, Department of Applied Chemistry, University of Johannesburg, Doornfontein Campus, P.O. Box 17011, Johannesburg, South Africa Tel: +27 11 559-6335 Fax: +27 11 559-6425

Competing Interest: The authors have declared that no competing interest exists.

Data Availability: All relevant data are within the paper and its supporting information files.

INTRODUCTION

Water availability has even become significantly important in this decade as the world tackles global climate changes with the need to provide cleaner water as the world population increases[1]. The year 2017 has seen a lot of fresh safe water scarcity in Southern Africa and other poor developing parts of the world. The decrease in annual rainfall and changes in weather patterns associated with global warming results in droughts related to El Nino[2]. Generally, El Nino is a phenomenon of prolonged warming of sea surface temperatures in the South Eastern African ocean (and other parts of the world) when compared with the usual value. Therefore, there is need to prevent existing fresh water from contamination with heavy metals and possible reclaiming of water contaminated by heavy metals.

The Cr(VI) is a metal ion that occurs naturally in rocks but is largely produced by industrial processes [3]. South Africa leads the global production of ferrochrome (FeCr)[4]. FeCr is a crude alloy of mainly iron and chromium, used largely in the production of stainless steel. Various FeCr production processes result in the generation of Cr(VI). According to Beukes *et al*., in 2012 there were fourteen separate FeCr smelters in South Africa, with a combined production capacity of over 4.7 metric tons/annum[4]. Cr(VI) is a highly toxic heavy metal found in industrial waste waters, which can cause health problems such as liver damage and pulmonary congestions[5]. The Environmental Protection Agency in 1990 set a maximum contaminant level of 0.05 mg L^{-1} for total chromium in drinking water [6]. The ease of solubility of these compounds in aqueous solutions makes them regular pollutants in the environment. Technologies such as ion exchange and chemical precipitation have been used to effectively reduce chromium concentrations from various aqueous solutions[7]. However, most of these methods require either high-energy or large quantities of chemicals[8] and are also characterized by high cost[9]. The heavy industrialization does not seem to be slowing down, hence, the need to find better, more efficient and effective methods of removing these heavy metals from water has arisen.

Activated carbons have been commonly used for the uptake of chromium from aqueous solutions[10-12], although their main challenge being poor efficiency when the metal ion concentration is low. The other drawback of activated carbons is their poor selectivity for a specific metal ion[13].

There has been a tremendous interest in carbon nanotubes (CNTs), ever since their discovery twenty years back. The potential application of the CNTs (either in the pristine or functionalized forms) as adsorbents for heavy metals has increasingly become very popular. Such potential applications are possible because of their characteristically small, hollow, layered structures which in turn gives them a large specific area[14]. Another advantage of CNTs which is sometimes overlooked is their ability to be regenerated[15].

Phosphonic acids are a class of organic compounds which play an important role as scale formation and corrosion inhibitors[16]. Furthermore, these compounds serve as ligands in metal complexation[17]. To date, different phosphorylating agents have been used to functionalize CNTs[18-21]. The resulting materials displayed new properties including magnetic[18], catalytic[19] and flame retardancy[20] that were exploited in various applications. Muleja *et al*.[22] phosphine functionalized CNTs that were applied in the removal of a heavy metal from aqueous solutions[23]. Oki *et al*.[21] reacted fluorinated CNTs with aminopropyl-phosphonic acid and subsequently dispersed them in silica by sol-gel processing, forming nanocomposites with potential use in bone tissue engineering. Cobalt and 4-chlorophenol were extracted from aqueous solution using phosphorylated MWCNTs[24]. Although, most authors have synthesized phosphorylated MWCNTs none of the materials were used as adsorbents for hexavalent chromium removal. This study aimed to report, the recovery of lowly concentrated Cr(VI) ions from aqueous solutions by using phosphorylated multiwalled carbon nanotubes (P-MWCNTs).

MATERIALS AND METHODS

Pristine MWCNTs (Pri-MWCNTs) with an outer diameter of 6-9 nm, length of 5 µm, purity of >95%, bulk density of 0.22 g cm^{-3}, true density of ~2.1 g mL^{-1} were purchased from Sigma Aldrich. All chemicals were analytical grade and used as received from Merck South Africa, including potassium dichromate (K Cr O). The 2-aminoethylphosphonic acid (AEPA), 99% purity, was sourced from Sigma Aldrich South Africa. Pri-MWCNTs were treated with acid to obtain the oxidized MWCNTs (O-MWCNTs).

Synthesis of oxidized MWCNTs: Oxidized MWCNTs were prepared according to the following: Pristine MWCNTs (2.00 g) were put into a one-neck round bottomed flask and H_2SO_4 (90 mL) and HNO_3 (30 mL) were added. The mixture was refluxed for 3 h at a temperature of 100°C (Fig. 1 summarises the oxidation procedure). After cooling to room temperature the O-MWCNTs were added to deionized water and vacuum filtered through a 0.45 µm PTFE membrane filter (Sigma S.A). The carbon nanotubes were repeatedly washed until a constant pH was reached. The sample was dried in an oven at

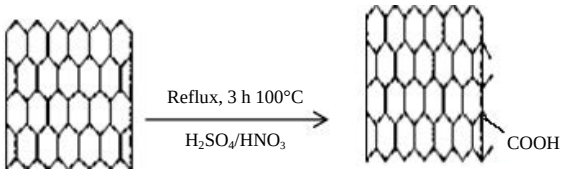

Fig. 1: Schematic diagram for oxidation of pristine carbon nanotubes

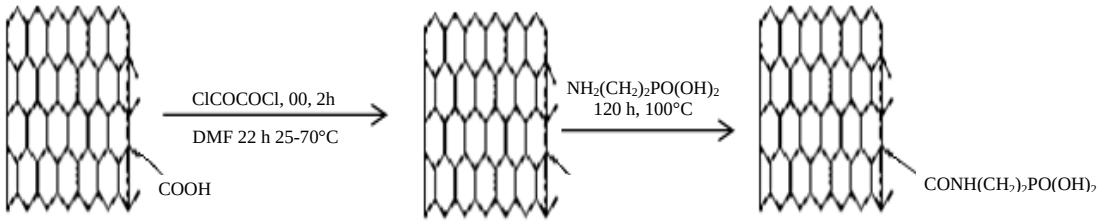

Fig. 2: Phosphorylation of oxidized carbon nanotubes

80°C for 24 h. Some of the O-MWCNTs kept aside for further use while the rest of O-MWCNTs were subsequently phosphorylated.

Phosphorylated MWCNTs synthesis: The P-MWCNTs were prepared according to the method of Mamba *et al.*[24] with minor modifications, that is, less of the O-MWCNTs were used 0.1 g instead of 0.8 g, more of the dimethylformamide solvent was used, 167 mL compared to 50 mL and finally the amount of oxalyl chloride was specified. These adjustments were found to produce effective yields of P-MWCNTs. The method was therefore as followed: A mixture of O-MWCNTs 0.1 g and dimethylformamide (DMF) (167 mL) was sonicated for 30 min. The mixture was fed into a 500 mL 3-neck round bottomed flask, cooled to 0°C and oxalyl chloride (1.0 mL) added dropwise. The suspension was stirred under reflux for 2 h. The cooling bath was removed and the reaction was allowed to progress for 2 more h at room temperature. The temperature was then raised to 70°C to remove the excess of oxalyl chloride and the reaction proceeded for 20 h. After 20 h, 2-aminoethylphosphonic acid (0.5 g) was added to the mixture, the temperature increased to 100 °C and the mixture stirred for 120 h. The mixture was then cooled to room temperature, filtered through a 0.45 µm membrane filter and washed with DMF and ethanol. The resulting residue was dried at 50°C under vacuum for 72 h. Yield 0.15 g, 150% (mass: mass) Fig. 2 summarizes the reactions.

Characterization of adsorbent: A Midac Fourier Transform Infrared (FTIR, model 4000, USA) spectroscopy was used to analyze the sample. A Perkin Elmer Pyris1 Thermal Gravimetric analyzer (TGA 4000, USA) was operated from a temperature of 30°C to a maximum temperature of 800°C and the samples were run under oxygen with a flow rate of 20 mL min^{-1}. The samples were also analysed using scanning electron microscopy (SEM) coupled with EDS. The micrographs were recorded using a JEOL JSM 7500F (USA). Brunauer-emmett-teller (BET) analysis was obtained at -198°C via N_2 adsorption/desorption according to the BET method using a Micromeritics TriStar (model ASAI2020, USA), surface area and porosity analyzer. The morphology of phosphorylated MWCNTs was determined by transmission electron microscopy (TEM model FEI Tecnai F30, USA).

Batch adsorption experiments: About 1000 ppm stock solution of Cr(VI) was prepared by dissolving 0.2874 g potassium dichromate in 100 mL deionized water. Through a series of dilution of the stock solution, a working solution of 0.1 ppm was obtained. Except for influence of pH experiments, all adsorption studies were carried at a pH of 7. This was chosen to simulate the pH of ground water (often found to be between 5 and 9)[25] and additionally above pH 7 precipitation occurs. All experiments (except for temperature effect) were conducted at room temperature (25±1 °C). The adsorption experiments were all done in triplicate.

Effect of adsorbent dosage on Cr(VI) adsorption: To investigate the effect of changing the amount of adsorbent on the removal of Cr(VI), 50 mL of 0.1 ppm ion solution was mixed together with adsorbent amount of between 2 and 50 mg in 100 mL conical flasks. The conical flasks were agitated at a speed of 120 revolutions per minute (rpm) using a mechanical shaker (Model 261, Merck, South Africa) for 120 min, after which the mixture was filtered through a 0.45 µm PTFE membrane filter.

Effect of contact time: A volume of 50 mL of the working solution of Cr(VI) was placed in a 100 mL conical flask. A mass of 10 mg of the adsorbent was weighed out and added to the flask. The conical flasks were agitated at a speed of 120 rpm using a mechanical shaker for contact times of 30, 60, 90, 120 and 150 min, respectively at room temperature. After the required contact time the adsorbent-ion mixture was filtered through a 0.45 µm PTFE membrane filter and the filtrate retained for analysis.

Effect of pH: The adsorbent, 10 mg, was placed in contact with 50 mL of 0.1ppm Cr(VI) solution in a 100 mL conical flask and either 0.1 M HNO_3 or 0.1 M NaOH solutions were used for pH adjustment. pH of 2, 3, 5, 7, 9, 11 and 13 were obtained, respectively. The adsorbent Cr(VI) ion mixture was allowed to equilibrate for 120 min at room temperature. Adsorption was facilitated by means of a shaker operated at 120 rpm. The mixture was then filtered using a PTFE membrane filter.

Effect of initial ion concentration: In order to carry out studies on the effect of Cr(VI) initial concentration on the adsorption uptake, 50 mL of Cr(VI) solutions with initial concentrations of 0.1-3.0 ppm were prepared and added to the 100 mL conical flasks. A mass of 10 mg of adsorbent was added to the solutions. The solution and adsorbent mixture was allowed to reach equilibrium after 120 min.

Effect of temperature: The Cr(VI) solution 50 mL, including adsorbent (10 mg) was shaken at 120 rpm for 120 min. The concentration was kept constant at 0.1ppm while temperature was varied at 30, 40, 50 and 60°C. The solution pH was also kept constant at 7. The contents of the flask were filtered through a 0.45 µm membrane and the filtrate retained for analysis.

Competing ions effect: The sulphate and chloride anions source were sodium sulphate and sodium chloride, respectively. The ions were selected as competing anions because they are often found in industrial effluent. Sulphate ions are almost chemically identical to dichromate ions. A concentration of 0.1 M was prepared for each ion. In a 100 mL conical flask, 50 mL of Cr(VI) were introduced and 10 mg of adsorbent added. The mixture was spiked with 10 mL sodium sulphate solution. The resulting mixture was agitated for 30, 60, 90, 120, 150 and 180 min, respectively before being filtered through a membrane filter. The procedure was repeated but 0.1 M sodium chloride used for spiking. The filtrates were again retained for analysis using UV-VIS Spectrophotometer.

Adsorbent regeneration: The adsorbents were first of all saturated with the metal ions. In a conical flask 10 mg of each adsorbent were weighed and 50 mL of 0.1 ppm Cr(VI) solution was added. The mixture was allowed to equilibrate at a pH = 7 for 4 h. After 4 h each sample was filtered through a 0.45 µm membrane and both the filtrate and residue retained for further analysis or use. Into another set of conical flask the adsorbent/Cr complex was introduced and either water or 1.0 M NaOH added. This was also agitated at 120 rpm for 5 h. Filtration then followed after which filtrate was analyzed for the amount of Cr(VI) present. The percentage desorption was calculated from the following equation[26]:

$$\text{Cr (VI) desorbed (\%)} = \frac{\text{Amount of ions desorbed from adsorbent}}{\text{Amount of ions adsorbed on to adsorbent}} \times 100 \quad (1)$$

Analysis of Cr(VI) content: All the retained filtrate was analyzed by a Shimadzu 2400 UV-VIS spectrophotometer (Japan) for the Cr(VI) content at 542 nm wavelength using 1,5 diphenylcarbazide as a complexing agent. The concentration of the Cr(VI) removed was then calculated using the following equations[27]:

$$\text{Cr (VI) removed (\%)} = \frac{(C_o - C_f)}{C_o} \times 100 \quad (2)$$

$$q_e = \frac{(C_0 - C_f)V}{m} \quad (3)$$

where, C_o and C_f are the initial and final Cr(VI) concentrations, respectively, V is the volume of Cr(VI) solution in liters and m is the weight of the adsorbent in grams. All adsorption experiments were done in triplicate and an average value was obtained.

Statistical analysis: To ensure that the data was reliable all batch adsorption experiments were carried out in triplicate. The standard deviation of the triple analytical data was determined and probability level used was $\leq$5%. Furthermore, blank experiments without the adsorbent were run concurrently with the adsorption experiments for the study. During the analysis of the residual Cr(VI) blank standards were also run. All the graphs were drawn using origin 8.0 software.

RESULTS AND DISCUSSION

Materials characterization: Figure S1 (supplementary data) shows the SEM image of the P-MWCNTs. The detailed

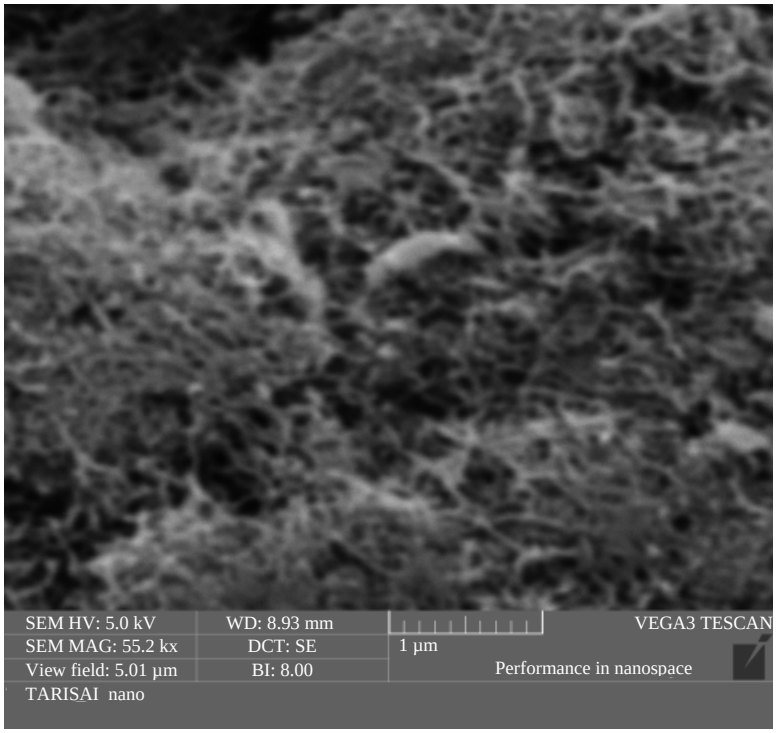

Fig. S1: SEM image of phosphorylated carbon nanotubes

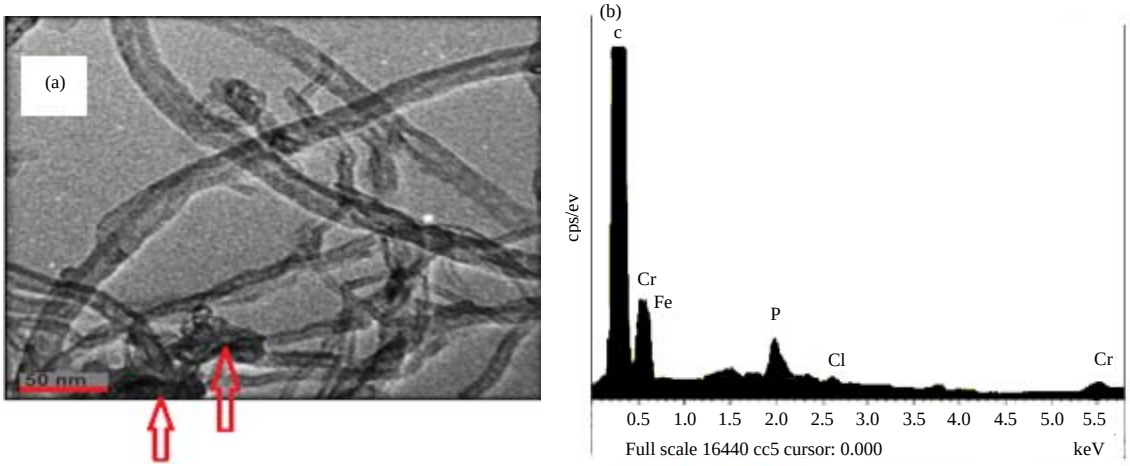

Fig. 3(a-b): (a) TEM images of P-MWCNTs (Arrows indicate expected tubular bundled MWCNTs) and (b) EDS of P-MWCNTs after Cr(VI) adsorption

morphology of the P-MWCNTs is however not noticeable from the SEM image, hence TEM analysis where done to obtain better morphologies of the P-MWCNTs.

The TEM image in Fig. 3a indicated the expected tubular bundled MWCNTs that are agglomerated. The agglomeration of MWCNTs can be attributed to intermolecular forces between MWCNTs of different sizes and direction. The surfaces of MWCNTs are coated with functional groups, darker areas in Fig. 3a (indicated by the arrows) can be due to the interconnection amongst the MWCNTs through the attached functional groups. The energy dispersive X-ray spectroscopy (EDS), confirmed presence of the Cr(VI) onto the adsorbent as presented by Fig. 3b. The predominant element is carbon as MWCNTs constituent of this element. The C element appears at an energy value of about 0.35 eV, while iron traces which originate from the catalyst employed during CNT synthesis and subsequently remained after functionalization appear at approximately 0.63 eV. Further evidence of phosphorylation

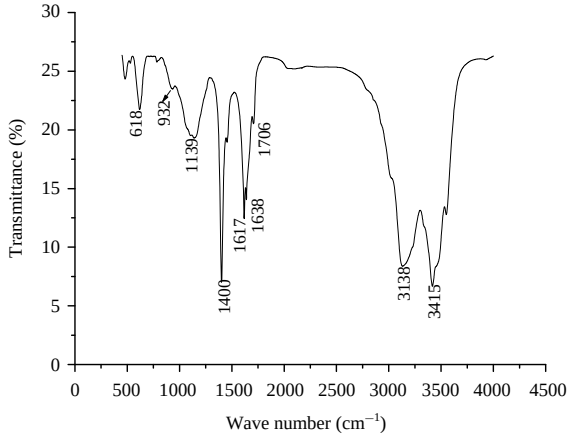

Fig. 4: FTIR spectrum of P-MWCNTs

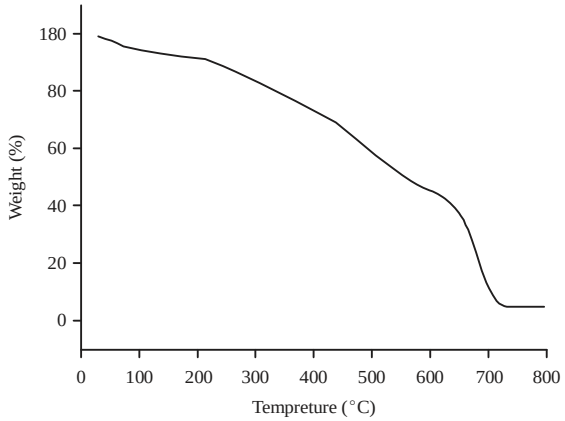

Fig. S2: TGA of P-MWCNTs

is displayed in Fig. 3b which has a significant phosphorous peak at 2.05 eV. Another element present is chlorine which is present at 2.61 eV. The chlorine was incorporated by substitution of the -OH functional groups during chlorination of O-MWCNTs using oxalyl chloride and further functionalization through phosphorylation did not remove the element, as illustrated by Eq. 4:

$$-\overset{|}{\underset{|}{C}}-OH \xrightarrow{\text{Oxalyl chloride}} -\overset{|}{\underset{|}{C}}-Cl \xrightarrow{\text{Amino phosphonic acid}} \text{no reaction} \quad (4)$$

The FTIR spectrum of phosphorylated MWCNTs (P-MWCNTs) is shown in Fig. 4. A peak at 3415 cm^{-1} refers to the O-H stretch of the hydroxyl group, which can be ascribed to the oscillation of carboxyl groups due to acidification carried before phosphorylation[22]. The peak at 1400 cm^{-1} is also associated with O-H bending deformation in carboxylic acids and phenolic groups[28]. Another conspicuous band is at 3138 cm^{-1}, corresponding to the C-H stretching vibrations. The presence of amino phosphonic acid functional group on the P-MWCNTs was confirmed by the appearance of bands at 932, 1139, 1706 and 3138 cm^{-1}. The peak at 932 cm^{-1} for P-MWCNTs is attributed to P-OH bond (Oki *et al.*[21], Zenobi *et al.*[29]. Also, the 1139 cm^{-1} band for P-MWCNTs can be due to the C-N bond Vukovic *et al.*[30] introduced through amidation of chlorinated carbon nanotubes by amino phosphonic acid. The carbon to nitrogen bond is known to appear in regions that can be related to some other functional groups. The band at 3138 cm^{-1} for P-MWCNTs is also related to the N-H stretch of the amide functional group, (-CONH-) which appears in the same region as C-H stretching vibrations mentioned above. Furthermore, a peak at 1706 cm^{-1} is as a result of the C=O functional group in the amide linkage, indicating that the phosphonic acid moiety was successfully attached to the MWCNTs.

The surface area determined by the BET method was found to be 131.7 $m^2 g^{-1}$ and pore volume was 1.07$cm^3 g^{-1}$. Functionalization led to a significantly lower pore volume compared to that of pristine (1.95 $cm^3 g^{-1}$) and O-MWCNTs (1.23 $cm^3 g^{-1}$). This decrease can be attributed to pore blockages by the functional groups. Comparing the surface area of pristine (255.9 $m^2 g^{-1}$), O-MWCNTs (244.5 $m^2 g^{-1}$) and P-MWCNTS there is a decrease in surface area with subsequent functionalization, contrary to another report[31] on pristine and O-MWCNTs. In any case oxidation introduced new defective sites and surfaces with defects are able to demonstrate high surface attraction of adsorbates[32].

The thermal stability of P-MWCNTs was investigated by TGA in an oxygen atmosphere and results are presented in Fig. S2. The weight loss at temperatures below 200°C, may be due to the elimination of water molecules[28]. Decomposition of functional groups, which include hydroxyl, carboxyl and amide was realized in the 200-500°C temperature range. The carbon nanotube skeleton decomposes at temperatures of 500-600°C. The remaining weight percentage was 5%. The CNTs were functionalized by an amino phosphonic acid and apparently, phosphonic acids can indirectly produce non-degradable residues (char)[16]. The decomposition of phosphonic acids has been shown to produce a number of products which include amino groups and phosphoric acid[33] and the phosphoric acid may have reacted on the surfaces of the carbon based material to produce the char which contributed to the overall remaining net weight of decomposed P-MWCNTs[34,35]. The char some how remained and contributed to a residual weight. The remaining 5% may also be due to remaining iron catalyst (as confirmed by EDS) which decomposes at higher temperatures.

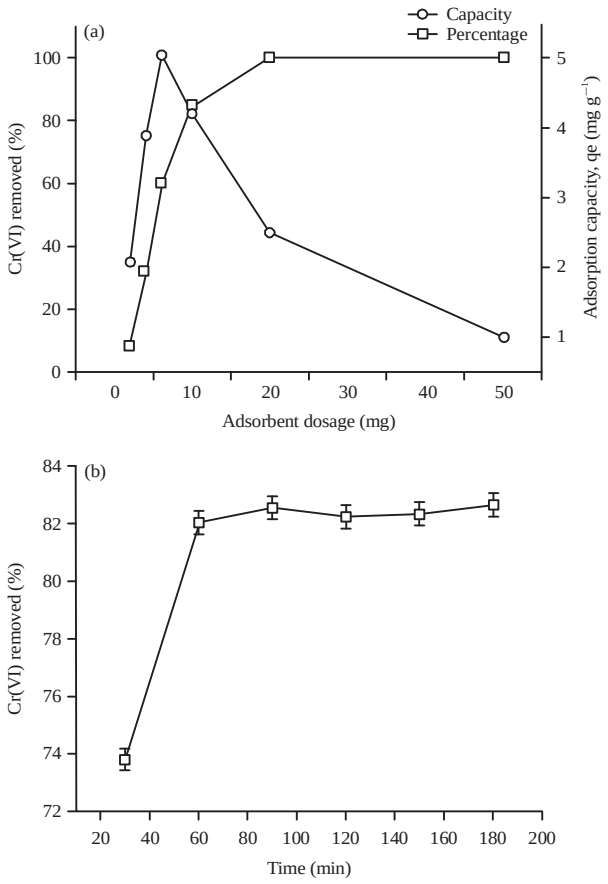

Fig. 5(a-b): (a) Effect of adsorbent dosage and (b) Contact time on the removal of Cr(VI)
Error bars represent the standard deviations for three triplicate adsorption experiment

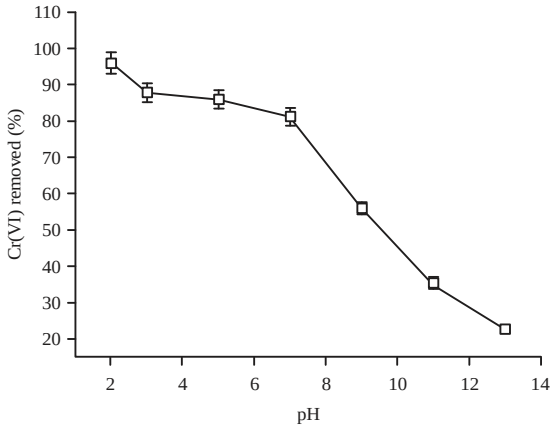

Fig. 6: pH influence on the removal of Cr(VI)
Error bars represent the standard deviations for three triplicate experiments

Effect of adsorbent dosage and contact time on Cr(VI) adsorption: The removal efficiency at various dosage amounts are as shown in Fig. 5a. It can be seen that the removal percentage increased with dosage increments up to 100% at 20 mg. The adsorption capacity increased to a maximum of 8 mg then decreased. Both graphs meet at 10 mg and this was established as the effective dose to use in this study.

The effect of contact time on chromium adsorption was observed at various contact time and the results indicated on Fig. 5b. A maximum adsorption percentage of 82% was reached after 90 min. Thereafter equilibrium was reached.

Influence of pH: The pH of a solution is an important factor on the adsorption process. It specifies the surface charge of adsorbent and consequently adsorption performance of heavy metals[36,37]. Adsorption trend revealed decreasing Cr(VI) uptake with an increase in pH as indicated in Fig. 6. It can be noticed that, the sorption process is highly pH dependent as 98% of Cr(VI) was removed at pH 5 and 56% at pH 9. Hexavalent chromium exists primarily as salts of hydrogen chromate ion ($HCrO_4^-$), chromate ion (CrO_4^{2-}) and chromic acid ($H_2CrO_7^-$), depending on the pH. The $H_2CrO_7^-$ species prevail at pH 2-1, at pH 1-7 $HCrO_4^-$ is predominate[38] pH 0-7.5, $Cr_2O_7^{2-}$ (dimer of $HCrO^-_4$) and CrO_4^{2-} exists between the pH of 7-10, although concentration tends to be low and negligible. Notably, across the pH ranges the species are all negatively charged. In acidic conditions protonation of the surfaces of the adsorbent with oxygen containing groups occurs[39-41]. As a result uptake of chromium can occur according to the illustration below:

$$CNT \cdot OH + H^+ \leftrightarrow CNT \cdot OH_2^+ + HCrO_4^- \leftrightarrow CNT \cdot OH_2CrO_4^- + H^+ \quad (5)$$

where, CNT-OH represents the adsorbent with OH group attached.

Chromium anions are attracted to the now positively charged surface of the adsorbents[42], hence the higher adsorption at lower pH. In addition to the oxygen functional groups, which were not phosphorylated, adsorption also takes place on the amino group:

$$-NH- + H^+ \leftrightarrow -NH_2^+ + HCrO_4^- \leftrightarrow -NH_2CrO_4^- + H^+ \quad (6)$$

At high pH values deprotonation occurs, due to a high concentration of negatively charged hydroxyl ions:

$$CNT{\cdot}OH \leftrightarrow CNT{\cdot}O^- + H^+ \quad (7)$$

$$-NH-(CH_2)_2P(O)(OH)_2 \leftrightarrow -NH-(CH_2)_2PO_3^{2-} + 2H^+ \quad (8)$$

The $HCrO_4^-$ anions are repelled by the more negative surface charge causing decrease in adsorption. Furthermore, at basic pH there is competition for the active sites of the adsorbent between the excess OH^- ions and Cr(VI) anions. However, referring to Fig. 6, adsorption of Cr(VI) was still relatively high in basic conditions for the CNTs adsorbents. At a pH above 8 precipitation of Cr(VI) ions in the form of $Cr(OH)_3$ occurs[43], thus at basic pH values precipitation rather than adsorption plays a major role in the anion removal from aqueous solution.

Another adsorption scenario of the Cr(VI) is the direct adsorption of the anions onto the surface of the adsorbent. The zeta potential was 4.2 (Fig. S3). Therefore, at a low pH, the MWCNTs are positively charged. Some workers also reported that MWCNTs are positively charged in acidic media[44]. However, this adsorption phenomenon is only applicable at low pH values. Also, in case of non-protonation and deprotonation Cr(VI) can interact with lone pair of electrons on nitrogen or oxygen by chelation (Fig. 7).

Initial ion concentration and temperature effect: The initial ion concentration effect on the uptake of Cr(VI) is shown in Fig. 8. The adsorption percentage decreases significantly until equilibrium as the chromium concentration increases. This can be attributed to the unavailability of adsorption sites. For all the experiments the amount of adsorbent used was the same, 10 mg, so the number of active sites remained the same[45]. At higher initial ion concentrations, the adsorption sites became saturated as more Cr(VI) anions compete for the constant number of active sites. Albadarin *et al.*[40] and Gupta and Balomajumder[46] observed similar results for the uptake of Cr(VI).

Amount of ions adsorbed increased with an increase in temperature (Fig. S4). Changes in solution temperature affect the way chromate anions are adsorbed because of the kinetic energy involved. The movement of the Cr ions towards the active sites increased thus encouraging greater adsorption. Adsorption increase with temperature was also due increase in the number of available active sites. As temperature increased destruction of a number of bonds which might have been blocking some active sites occurred[46].

Adsorption kinetics: Adsorption kinetics of any adsorption processes are applied in the description of mass transfers and chemical reaction that occur.

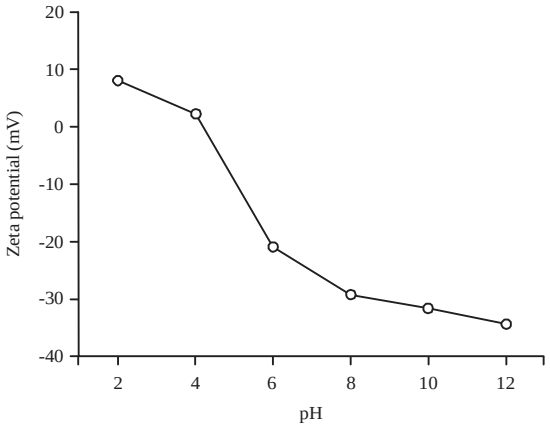

Fig. S3: Zeta potential of P-MWCNTs

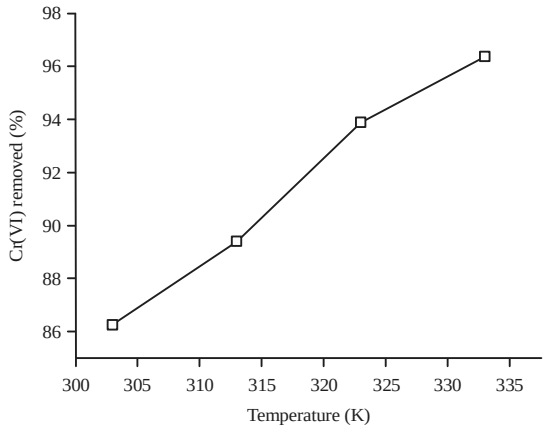

Fig. S4: Effect of temperature on Cr(VI) removal

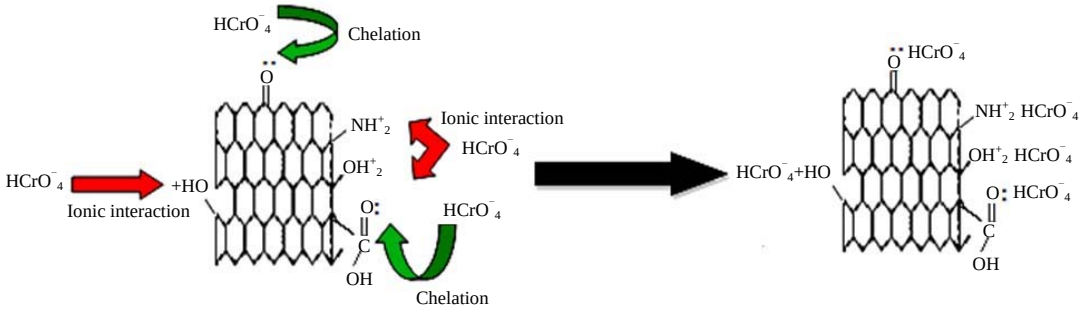

Fig. 7: Possible uptake process of Cr(VI) from aqueous solution

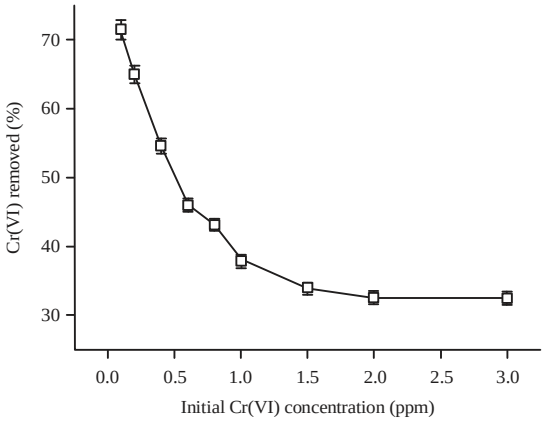

Fig. 8: Effect of initial ion concentration on the adsorption uptake
Error bars represent the standard deviations for three triplicate adsorption experiments

The pseudo-first-order is represented by the equation:

$$\log(q_e - q_t) = \log q_e - \frac{k_1}{2.303}t \quad (9)$$

The pseudo second order equation is given as:

$$\frac{t}{q_t} = \frac{1}{k_2 q_e^2} + \frac{1}{q_e}t \quad (10)$$

where, q_e (mg g^{-1}) and q_t (mg g^{-1}) are the amount of metal ion adsorbed at equilibrium and time, t(h)/unit weight of the sorbent, respectively. The linear plots of the pseudo-first-order and pseudo-second-order kinetics are represented in Fig. 9a and b, respectively.

A plot of t/q_t should give a straight line if pseudo second order is relevant. Pseudo second order plot is indicated in Fig. 9b. The pseudo-second-order proposes that adsorption process occurs in a chemisorption manner[47]. The correlation co-efficient was excellent, clearly showing that the adsorption follows the pseudo-second-order model. Moreover, q calculated (q_{cal}) is consistent with q experimental (q_{exp}), refer to Table S1. The results are in agreement with findings on Cr(VI) adsorption[41,48].From Table S1 the correlation coefficient value of pseudo-first-order was very poor therefore reaction does not follow first order kinetics.

Generally, overall rate of adsorption process is controlled by either surface diffusion or intraparticle diffusion. The adsorption process may occur through firstly, adsorbate transportation from the bulk solution to the exterior surface of adsorbent, secondly rapid adsorbate particle adsorption to the

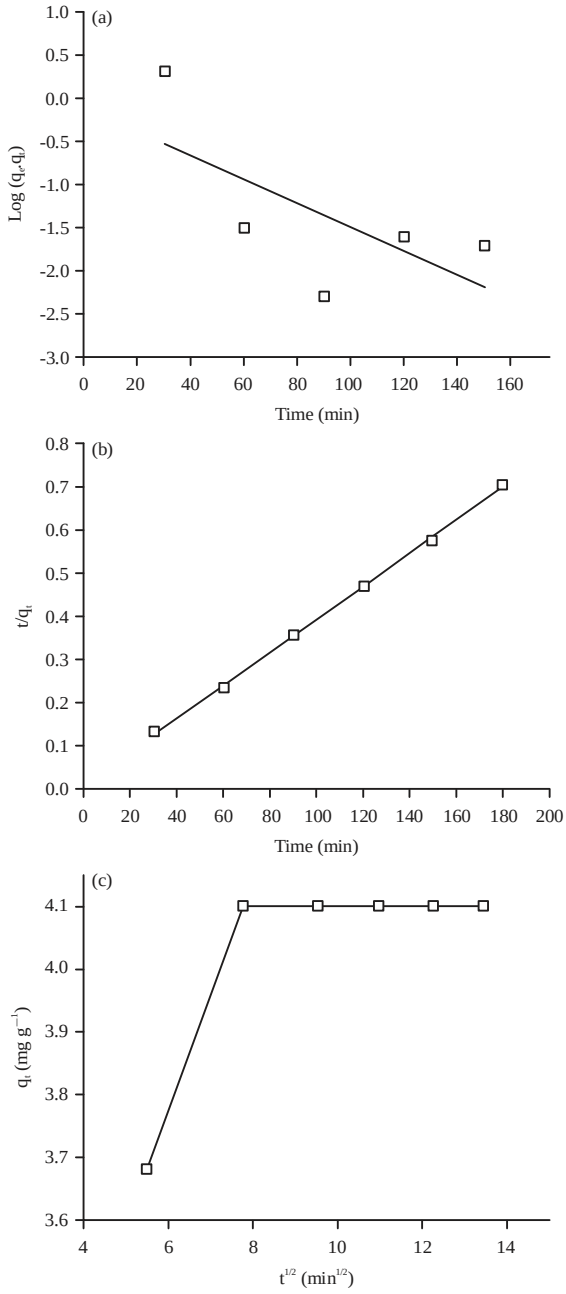

Fig. 9(a-c): Showing Kinetic parameters (a) Pseudo-first-order (b) Pseudo-second-order and (c) Weber–Morris intraparticle diffusion model

interior or exterior site surface of adsorbent and thirdly surface diffusion or pore diffusion of adsorbate particles adsorption site. To determine if intraparticle diffusion is the rate-limiting step[49] in an adsorption system, the Weber-Morris intraparticle diffusion model has often been used and represented by Eq. 11:

$$q_t = k_p t^{1/2} + C \quad (11)$$

Table S1: Pseudo-first-orderand second-order kinetic parameters for Cr(VI)adsorption

2nd order						1st order		
Time (min)	q_e (exp) (mg g^{-1})	q_e (cal) (mg g^{-1})	$k_2 \times 10^{-3}$ (g mg^{-1} min^{-1})	h (mg g^{-1} min^{-1})	R^2	q_e (mg g^{-1})	$k_1 \times 10^{-2}$ (min^{-1})	R^2
60	4.9	4.2	1.24	78.68	0.999	0.916	3.47	0.699

Table 1: Comparison of P-MWCNTs uptake at low concentrations with other adsorbents

Adsorbent	Concentration range (mg L^{-1})	Adsorption capacity q_m (mg g^{-1})	Reference
Oak wood char	1-100	3.03	Jung[11]
Oxidized MWCNTs	1-10	4.20	Albadarin *et al.*[40]
Modified Sand	1-5	0.79	Yadav *et al.*[53]
P-MWCNTs	0.1-3	4.35	Present study

A plot of q_t versus $t^{1/2}$ should be linear if intraparticle diffusion is involved in the adsorption process and the deviation of the line from the origin further shows than that intraparticle transport is not the only rate limiting step[50]. This implies that adsorption is affected by more than one process. Figure 9cis the plot of q_t vs. $t^{1/2}$ which indicates that the plot of qt vs. $t^{1/2}$ had two linear portions. The initial portion represents film or external diffusion where adsorbate moves from liquid phase to the adsorbent surface and the second portion is due to intraparticle diffusion. However, adsorption processes of the three elements are comprised of two stages, suggesting that the intraparticle diffusion is not the rate-limiting step for the entire reaction[51].

Adsorption isotherms: Freundlich and Langmuir are models often used to describe the adsorption and distribution of a metal ion between a solid and a liquid phase ion. The linear form of the Langmuir equation is given as:

$$\frac{Ce}{Qe} = \frac{1}{q_m b} + \frac{Ce}{q_m} \quad (12)$$

Ce represents the equilibrium concentration of the ion in aqueous solution, Qe is the adsorption capacity of the adsorbent, that is, the amount of adsorbate per unit mass adsorbent and both b, q_m are the constants. The factor b describes the affinity of the surface for the solute and corresponds to the energy of adsorption. The constant q_m is related to adsorption efficiency.

The Langmuir plot of Co/Qe against Co, where Co is the initial ion concentration as illustrated by Fig. 10a. The correlation coefficient was 0.975 for the adsorbent indicating that the Langmuir isotherm fits well with a q_m value of 4.35 mg g^{-1} and b value of 0.73 L mg^{-1}. Of noteworthy importance is that for comparison purposes between the adsorbents, (Co) was used instead of Ce for both isotherm calculations.

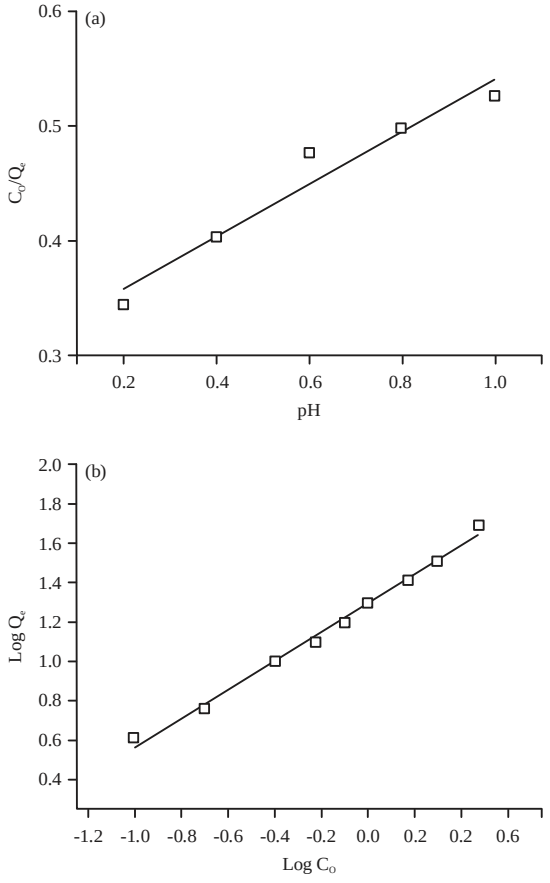

Fig. 10(a-b): Adsorption Isotherms (a) Langmuir and (b) Freundlich

The adsorption data were also fitted to the Freundlich model given in Eq. 13:

$$\log Qe = \frac{1}{n}\log Ce + \log K \quad (13)$$

where, Qe is the adsorption capacity, Ce is the equilibrium concentration of adsorbate in solution, K and 1/n are constants depicting adsorption capacity and adsorption

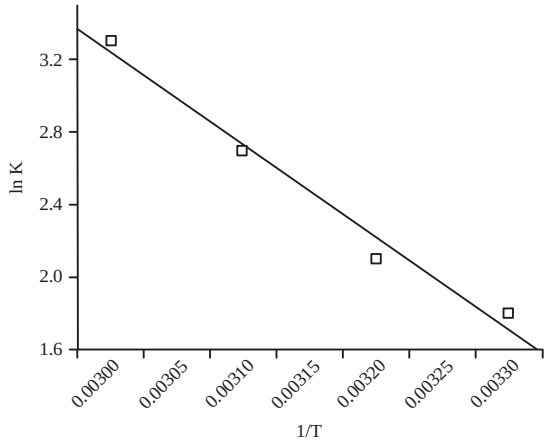

Fig. 11: Plot of Van't Hoff, thermodynamic parameters determination

Table 2: Thermodynamic parameters for the adsorption of Cr(VI) onto phosphorylated multiwalled carbon nanotubes

Temperature(K)	ΔG° (kJ mol^{-1})	ΔH° (kJ mol^{-1})	ΔS° (kJ mol^{-1} K^{-1})
303	-4.53	42.3	0.153
313	-5.46	-	-
323	-7.24	-	-
333	-9.12	-	-

intensity, respectively. The values of 1/n that vary between 0.1 and 1.0 indicate the favourable adsorption of heavy metals[52]. From Fig. 10b, the plots produced were linear with an R^2 value of 0.997. The intercept, K and slope 1/n were deduced from the graphs and were 1.95 and 0.73 mg g^{-1}, respectively.

Previous findings of the adsorption capacities based on the Cr(VI) concentrations applied are summarized in Table 1. The P-MWCNTs are still effective as adsorbents because adsorption capacity was higher although ion concentrations applied in this study were lower compared to other studies.

Adsorption thermodynamics: The Vant Hoff equation (Eq. 14) is used to calculate the thermodynamic parameters, standard free energy (G°), standard enthalpy (H°) and standard entropy (S°) as depicted in Fig. 11:

$$\ln K = \frac{-H^O}{RT} + \frac{S^O}{R} \quad (14)$$

$$\Delta G = -RT \ln K \quad (15)$$

In this case K is obtained from the ratio of adsorbate particles attached to the surface of the adsorbent to that of the adsorbate particles in the aqueous solution. R is the gas constant (J K^{-1} mol^{-1}), T is the temperature (Kelvin). Figure 10 is a straight line plot of ln K versus 1/T and the parameters H° and S° were calculated from the slope and intercept, respectively.

The enthalpy change, H° was positive (endothermic) due to increase in adsorption on successive increase in temperature as indicated in Table 2. Furthermore, negative G° values reveal the spontaneous nature of the adsorption process. A positive value of S° shows the increased randomness at the adsorbent/solution interface during the Cr(VI) adsorption on the active sites of the adsorbent.

Effect of competing ions: The SO_4^{2-} and Cl^- anions effect on the adsorption capacity of Cr(VI) was investigated by spiking the Cr(VI) solutions with sodium sulfate and sodium chloride, respectively. More Cr(VI) ions were adsorbed in the presence of chloride ions (69%) compared to sulfate ions (56%). Sulfate ions and dichromate ions have similar charge density[45] causing direct competition for adsorbent active sites. The adsorption pattern resembles previous results observed in the selectivity effect of A.C for Cr(VI) in the presence of sulfate and chloride ions[54]. According to Duranoglu *et al.*[54], Cl^- ions absorb better to water molecules than chromium ions in the form of chromic acid ($HCrO_4^-$) making their uptake less favorable to the hydrophobic surface of carbon.

Desorption study: As previously reported, the acidic conditions were best for adsorption, therefore, alkali and neutral conditions were selected for desorbing chromium ions. The percentage of Cr(VI) desorbed was determined as 87% after treating the adsorbent/Cr mixture with 0.1 M NaOH. According to Saleh and Gupta[55] adsorbent pores are divided into three classes: Macropores (width <50 nm), mesopores (2 nm<width>50 nm), category and micropores (width<2 nm). Of great importance in Cr(VI) adsorption is both the micropores and mesopores of an adsorbent whereas desorption relies more on the mesoporosity[13], that is, the higher the mesoporosity of an adsorbent, the easier to desorb metal ions. Generally, mesopore size of MWCNTs is 2-50 nm[56] and it is quiet high, hence desorption would be favourable.

CONCLUSION

The P-MWCNTs were produced through the treatment of carboxylic acid of O-MWCNTs with oxalyl chloride followed by amidation with 2-amino ethyl phosphonic acid. The FTIR confirmed the grafting of organophosphonic acid moieties with the appearance of an amide bond. P-MWCNTs revealed

good selectivity for Cr(VI) and excellent adsorption efficiency at low concentrations applied in this study. Furthermore, P-MWCNTs can be reused without loss of efficiency and can therefore find practical use in the uptake of lowly concentrated Cr(VI) aqueous containing other anions.

SIGNIFICANCE STATEMENT

This study reported the synthesis of a new adsorbent made of multiwalled carbon nanotube decorated with phosphonic acid moieties (P-MWCNTs). The new P- MWCNTs adsorbent can selectively remove Cr(VI) from water at very low concentration.

ACKNOWLEDGMENT

The authors would like to thank the University of Johannesburg, Faculty of Science for funding (URC/210-2016).

REFERENCES

1. O'Leary, M., 2011. Your Water Footprint is Next. In: Sustainability in the Chemistry Curriculum, Middlecamp, C.H. and A.D. Jorgensen (Eds.). Vol. 1087, American Chemical Society, USA., pp: 175-186.
2. Nordstrom, D.K., 2009. Acid rock drainage and climate change. J. Geochem. Expl., 100: 97-104.
3. Jacobs, J.A. and S.M. Testa, 2004. Overview of Chromium (VI) in the Environment: Background and History. In: Chromium (VI) Handbook, Guertin, J., J.A. Jacobs and C.P. Avakian (Eds.). CRC Press, Boca Raton, FL.
4. Beukes, J.P., P.G. van Zyl and M. Ras, 2012. Treatment of Cr (VI)-containing wastes in the South African ferrochrome industry-a review of currently applied methods. J. Southern Afr. Inst. Mining Metallurgy, 112: 347-352.
5. Shechan, P.J., D.M. Meyer, M.M. Sauer and D.J. Paustenbach, 1991. Assessment of the human health risks posed by exposure to chromium contaminated soils. J. Toxicol. Environ. Health, 32: 161-201.
6. Ballav, N., A. Maity and S.B. Mishra, 2012. High efficient removal of chromium (VI) using glycine doped polypyrrole adsorbent from aqueous solution. Chem. Eng. J., 198-199: 536-546.
7. Hawley, E.L., R.A. Deeb, M.C. Kavanaugh and R.G. James Jacobs, 2004. Treatment Technologies for Chromium (VI). In: Chromium (VI) Handbook, Guertin, J., J.A. Jacobs and C.P. Avakian (Eds.). CRC Press, Boca Raton, FL.
8. Mohan, D., S. Rajput, V.K. Singh, P.H. Steele and C.U. Pittman, Jr., 2011. Modeling and evaluation of chromium remediation from water using low cost bio-char, a green adsorbent. J. Hazardous Mater., 188: 319-333.
9. Gupta, V.K., R. Jain, A. Mittal, T.A. Saleh, A. Nayak, S. Agarwal and S. Sikarwar, 2012. Photo-catalytic degradation of toxic dye amaranth on TiO_2/UV in aqueous suspensions. Mater. Sci. Eng.: C, 32: 12-17.
10. Al-Othman, Z.A., R. Ali and M. Naushad, 2012. Hexavalent chromium removal from aqueous medium by activated carbon prepared from peanut shell: Adsorption kinetics, equilibrium and thermodynamic studies. Chem. Eng. J., 184: 238-247.
11. Jung, C., J. Heo, J. Han, N. Her and S.J. Lee *et al*., 2013. Hexavalent chromium removal by various adsorbents: Powdered activated carbon, chitosan and single/multi-walled carbon nanotubes. Sep. Purif. Technol., 106: 63-71.
12. ALOthman, Z.A., M. Naushad and R. Ali, 2013. Kinetic, equilibrium isotherm and thermodynamic studies of Cr (VI) adsorption onto low-cost adsorbent developed from peanut shell activated with phosphoric acid. Environ. Sci. Pollut. Res., 20: 3351-3365.
13. Mohan, D. and C.U. Pittman, Jr., 2006. Activated carbons and low cost adsorbents for remediation of tri-and hexavalent chromium from water. J. Hazard. Mater., 137: 762-811.
14. Peigney, A., C. Laurent, E. Flahaut, R.R. Bacsa and A. Rousset, 2001. Specific surface area of carbon nanotubes and bundles of carbon nanotubes. Carbon, 39: 507-514.
15. Ji, L., Y. Shao, Z. Xu, S. Zheng and D. Zhu, 2010. Adsorption of monoaromatic compounds and pharmaceutical antibiotics on carbon nanotubes activated by KOH etching. Environ. Sci. Technol., 44: 6429-6436.
16. Amar, H., J. Benzakour, A. Derja, D. Villemin and B. Moreau, 2003. A corrosion inhibition study of iron by phosphonic acids in sodium chloride solution. J. Electroanal. Chem., 558: 131-139.
17. Lacour, S., V. Deluchat, J.C. Bollinger and B. Serpaud, 1998. Complexation of trivalent cations (Al(III), Cr(III), Fe(III)) with two phosphonic acids in the pH range of fresh waters. Talanta, 46: 999-1009.
18. Jin, X., B. He, J. Miao, Q. Zhang and L. Niu, 2012. Stabilization and dispersion of PtRu and Pt nanoparticles on multiwalled carbon nanotubes using phosphomolybdic acid and the use of the resulting materials in a direct methanol fuel cell. Carbon, 50: 3083-3091.
19. Zhang, Y., S. Qi and F. Zhang, 2012. Preparation and characterization of multi-walled carbon nanotubes with nickel–phosphorous layers of high magnetic properties. Mater. Res. Bull., 47: 3743-3746.
20. Gashti, M.P. and A. Almasian, 2013. UV radiation induced flame retardant cellulose fiber by using polyvinylphosphonic acid/carbon nanotube composite coating. Composites Part B: Eng., 45: 282-289.
21. Oki, A., L. Adams, V. Khabashesku, Y. Edigin, P. Biney and Z. Luo, 2008. Dispersion of aminoalkylsilyl ester or amine alkyl-phosphonic acid side wall functionalized carbon nanotubes in silica using sol-gel processing. Mater. Lett., 62: 918-922.

22. Muleja, A.A., X.Y. Mbianda, R.W. Krause and K. Pillay, 2012. Synthesis, characterization and thermal decomposition behaviour of triphenylphosphine-linked multiwalled carbon nanotubes. Carbon, 50: 2741-2751.
23. Adolph, M.A., Y.M. Xavier, P. Kriveshini and K. Rui, 2012. Phosphine functionalised multiwalled carbon nanotubes: A new adsorbent for the removal of nickel from aqueous solution. J. Environ. Sci., 24: 1133-1141.
24. Mamba, G., X.Y. Mbianda and P.P. Govender, 2013. Phosphorylated multiwalled carbon nanotube-cyclodextrin polymer: Synthesis, characterisation and potential application in water purification. Carbohydrate Polymers, 98: 470-476.
25. Lv, X., J. Xu, G. Jiang and X. Xu, 2011. Removal of chromium(VI) from wastewater by nanoscale zero-valent iron particles supported on multiwalled carbon nanotubes. Chemosphere, 85: 1204-1209.
26. Deb, A.K.S., V. Dwivedi, K. Dasgupta, S.M. Ali and K.T. Shenoy, 2017. Novel amidoamine functionalized multi-walled carbon nanotubes for removal of mercury (II) ions from wastewater: Combined experimental and density functional theoretical approach. Chem. Eng. J., 313: 899-911.
27. Kera, N.H., M. Bhaumik, N. Ballav, K. Pillay, S.S. Ray and A. Maity, 2016. Selective removal of Cr(VI) from aqueous solution by polypyrrole/2,5-diaminobenzene sulfonic acid composite. J. Colloid Interface Sci., 476: 144-157.
28. Xu, J., P. Yao, X. Li and F. He, 2008. Synthesis and characterization of water-soluble and conducting sulfonated polyaniline/*para*-phenylenediamine-functionalized multi-walled carbon nanotubes nano-composite. Mater. Sci. Eng.: B, 151: 210-219.
29. Zenobi, M.C., C.V. Luengo, M.J. Avena and E.H. Rueda, 2008. An ATR-FTIR study of different phosphonic acids in aqueous solution. Spectrochim. Acta Part A: Mol. Biomol. Spectroscopy, 70: 270-276.
30. Vukovic, G.D., A.D. Marinkovic, M. Colic, M.D. Ristic, R. Aleksic, A.A. Peric-Grujic and P.S. Uskokovic, 2010. Removal of cadmium from aqueous solutions by oxidized and ethylenediamine-functionalized multi-walled carbon nanotubes. Chem. Eng. J., 157: 238-248.
31. Saleh, T.A. and V.K. Gupta, 2012. Photo-catalyzed degradation of hazardous dye methyl orange by use of a composite catalyst consisting of multi-walled carbon nanotubes and titanium dioxide. J. Colloid Interface Sci., 371: 101-106.
32. Gupta, V.K., R. Kumar, A. Nayak, T.A. Saleh and M.A. Barakat, 2013. Adsorptive removal of dyes from aqueous solution onto carbon nanotubes: A review. Adv. Colloid Interface Sci., 193-194: 24-34.
33. Jiang, D.D., Q. Yao, M.A. McKinney and C.A. Wilkie, 1999. TGA/FTIR studies on the thermal degradation of some polymeric sulfonic and phosphonic acids and their sodium salts. Polymer Degrad. Stability, 63: 423-434.
34. Fierro, V., V. Torne-Fernandez and A. Celzard, 2006. Kraft lignin as a precursor for microporous activated carbons prepared by impregnation with ortho-phosphoric acid: Synthesis and textural characterisation. Microporous Mesoporous Mater., 92: 243-250.
35. Hayashi, J., A. Kazehaya, K. Muroyama and A.P. Watkinson, 2000. Preparation of activated carbon from lignin by chemical activation. Carbon, 38: 1873-1878.
36. Gupta, V.K., S. Agarwal and T.A. Saleh, 2011. Synthesis and characterization of alumina-coated carbon nanotubes and their application for lead removal. J. Hazard. Mater., 185: 17-23.
37. Li, K., P. Li, J. Cai, S. Xiao, H. Yang and A. Li, 2016. Efficient adsorption of both methyl orange and chromium from their aqueous mixtures using a quaternary ammonium salt modified chitosan magnetic composite adsorbent. Chemosphere, 154: 310-318.
38. Petersen, E.J., J. Akkanen, J.V.K. Kukkonen and W.J. Weber, Jr., 2009. Biological uptake and depuration of carbon nanotubes by *Daphnia magna*. Environ. Sci. Technol., 43: 2969-2975.
39. Hu, J., C. Chen, X. Zhu and X. Wang, 2009. Removal of chromium from aqueous solution by using oxidized multiwalled carbon nanotubes. J. Hazardous Mater., 162: 1542-1550.
40. Albadarin, A.B., A.H. Al-Muhtase, G.M. Walker, S.J. Allen and M.N.M. Ahmad, 2011. Retention of toxic chromium from aqueous phase by H_3PO_4-activated lignin: Effect of salts and desorption studies. Desalination, 274: 64-73.
41. Giraldo-Gutierrez, L. and J.C. Moreno-Pirajan, 2008. Pb(II) and Cr(VI) adsorption from aqueous solution on activated carbons obtained from sugar cane husk and sawdust. J. Anal. Applied Pyrolysis, 81: 278-284.
42. Park, S.J., B.J. Park and S.K. Ryu, 1999. Electrochemical treatment on activated carbon fibers for increasing the amount and rate of Cr(VI) adsorption. Carbon, 37: 1223-1226.
43. Kotas, J. and Z. Stasicka, 2000. Chromium occurrence in the environment and methods of its speciation. Environ. Pollut., 107: 263-283.
44. Lu, C. and H. Chiu, 2006. Adsorption of Zinc(II) from water with purified carbon nanotubes. Chem. Eng. Sci., 61: 1138-1145.
45. Pillay, K., E.M. Cukrowska and N.J. Coville, 2009. Multi-walled carbon nanotubes as adsorbents for the removal of parts per billion levels of hexavalent chromium from aqueous solution. J. Hazardous Mater., 166: 1067-1075.
46. Gupta, A. and C. Balomajumder, 2015. Simultaneous adsorption of Cr(VI) and phenol onto tea waste biomass from binary mixture: Multicomponent adsorption, thermodynamic and kinetic study. J. Environ. Chem. Eng., 3: 785-796.
47. Chen, J., N. Xia, T. Zhou, S. Tan, F. Jiang and D. Yuan, 2009. Mesoporous carbon spheres: Synthesis, characterization and supercapacitance. Int. J. Electrochem. Sci., 4: 1063-1073.

48. Sharma, D.C. and C.F. Forster, 1996. Removal of hexavalent chromium from aqueous solutions by granular activated carbon. Water SA., 22: 153-160.
49. Wu, F.C., R.L. Tseng and R.S. Juang 2009. Initial behavior of intraparticle diffusion model used in the description of adsorption kinetics. Eng. J., 153: 1-8.
50. Kapur, M. and M.K. Mondal, 2013. Mass transfer and related phenomena for Cr(VI) adsorption from aqueous solutions onto *Mangifera indica* sawdust. Chem. Eng. J., 218: 138-146.
51. Hu, X.J., J.S. Wang, Y.G. Liu, X. Li and G.M. Zeng *et al*., 2011. Adsorption of chromium (VI) by ethylenediamine-modified cross-linked magnetic chitosan resin: Isotherms, kinetics and thermodynamics. J. Hazardous Mater., 185: 306-314.
52. Unnithan, M.R. and T.S. Anirudhan, 2001. The kinetics and thermodynamics of sorption of chromium(VI) onto the iron(III) complex of a carboxylated polyacrylamide-grafted sawdust. Ind. Eng. Chem. Res., 40: 2693-2701.
53. Yadav, S., V. Srivastava, S. Banerjee, C.H. Weng and Y.C. Sharma, 2013. Adsorption characteristics of modified sand for the removal of hexavalent chromium ions from aqueous solutions: Kinetics, thermoynamic and equilibrium studies. Catena, 100: 120-127.
54. Duranoglu, D., A.W. Trochimczuk and U. Beker, 2012. Kinetics and thermodynamics of hexavalent chromium adsorption onto activated carbon derived from acrylonitrile-divinylbenzene copolymer. Chem. Eng. J., 187: 193-202.
55. Saleh, T.A. and V.K. Gupta, 2014. Processing methods, characteristics and adsorption behavior of tire derived carbons: A review. Adv. Colloid Interface Sci., 211: 93-101.
56. Jagtoyen, M., J. Pardue, T. Rantell, E. Grulke and F. Derbyshire, 2000. Porosity of Carbon Nanotubes. Vol. 45, American Chemical Society, USA., pp: 908-911.